AUV IDENTIFICATION BY USE OF SELF-OSCILLATIONS

Nikola Miskovic[1], Zoran Vukic[1], Matko Barisic[1] and Philip P. Soucacos[2]
[1] Faculty of Electrical Engineering and Computing,
University of Zagreb, Unska 3, 10000 Zagreb, Croatia
[2] CSSI, Inc., 400 Virginia Ave., SW, Ste. 210, Washington D.C., USA
E-mail: nikola.miskovic@fer.hr

Abstract: Given the fact that AUV dynamics change depending on the payload, finding a mathematical model in a rather small period of time is quite important. Classical open-loop identification methods give accurate parameter identification, but are also time consuming. In the paper we present an identification method based on induced self-oscillations, which has proved to be applicable to underwater vehicles. In addition to that, an error analysis for the proposed method is presented. Experimental results obtained on an underwater vehicle are given and compared to the results obtained using open-loop identification algorithms. *Copyright © 2007 IFAC*

Keywords: underwater vehicle, parameter identification, self-oscillations, limit cycles

1. INTRODUCTION

The control of marine vehicles presents a challenging task, mostly due to complex mathematical models that describe their motion. The main characteristics of their dynamics are high coupling and nonlinear effects. In addition to that, 6 DOF make the control even more complex. Prior to control development for any type of system, a proper mathematical model has to be identified. Usually, this is a complex task that requires numerous experiments. This paper presents a new method based on identification by use of self-oscillations for determining ROV or AUV mathematical model parameters. The general identification algorithm given in detail in (Miskovic et. al. 2007b) is used for the ROV yaw linear model, and a modification of the algorithm for identification of the nonlinear mathematical models is presented.

The paper is organized as follows. Section 2 gives the proposed identification algorithm procedure for linearized and nonlinear mathematical model of the ROV's yaw dynamics. Section 3 gives error analysis based on simulations together with recommendations for performing experiments on real systems. Section 4 presents experimental results obtained on a real system, and the paper is concluded with Section 5.

1.1. Some Prior Work

Methods for identification of marine vehicles' dynamics can be found in literature, e.g. by Carreras M. et al. (2003), Ridao *et al.*, (2004), and by M. Caccia *et al.*, (1998), (2000). While Caccia uses classical measured data and some estimations to obtain the model of *Charlie* (autonomous surface catamaran), Carreras designed a uniquely patterned bottom of a laboratory test pool in order to localize *Uris* (unmanned underwater vehicle) and thus calculate the speeds which are necessary for model identification. Both authors use either linearized vehicle models, or "zig-zag" maneuvers to determine some model parameters. Stipanov *et al.* (2007) give a method for open-loop identification where open-loop system response is used to determine all parameters of the nonlinear system. Coupled mathematical model identification can also be found in (Miskovic *et al.*, (2007a)).

1.2. Underwater Vehicles' Mathematical Model

Marine vehicles' mathematical models consist of kinematic and dynamic part. The kinematic model gives the relation between speeds in a body-fixed frame and derivatives of positions and angles in an Earth-fixed frame, (Fossen, 1994). According to terminology in (Fossen, 1994), vector of positions and angles of an underwater vehicle ${}^{E}\boldsymbol{\eta} = [x \quad y \quad z \quad \varphi \quad \theta \quad \psi]^T$ is defined in the Earth-fixed coordinate system (E) and vector of linear and angular velocities ${}^{B}\mathbf{v} = [u \quad v \quad w \quad p \quad q \quad r]^T$ (surge, sway, heave, roll, pitch and yaw velocity, respectively) is defined in a body-fixed (B) coordinate system.

As stated before, the dynamic model of underwater vehicles is highly coupled and nonlinear. The main reasons for this are not only the rigid-body dynamics but hydrodynamic influences also. A general dynamic equation for underwater vehicles is given with (2).

$$\mathbf{M}\dot{\mathbf{v}} + \mathbf{C}(\mathbf{v})\mathbf{v} + \mathbf{D}(\mathbf{v})\mathbf{v} + \mathbf{g}(\boldsymbol{\eta}) = \boldsymbol{\tau} + \boldsymbol{\tau}_d \qquad (2)$$

Matrix $\mathbf{M} = \mathbf{M}_{RB} + \mathbf{M}_A$ represents the sum of the rigid-body mass and added mass matrix. Matrix $\mathbf{D}(\mathbf{v})$ is a damping matrix, which is diagonal and usually represented with a linear and/or quadratic term. Matrix $\mathbf{C}(\mathbf{v}) = \mathbf{C}_{RB}(\mathbf{v}) + \mathbf{C}_A(\mathbf{v})$ represents the sum of the rigid-body and added mass Coriolis matrix, vector $\mathbf{g}$ represents gravitational and buoyancy forces, vector $\boldsymbol{\tau}$ consists of external forces and moments that act upon the underwater vehicle and $\boldsymbol{\tau}_d$ is the disturbance vector.

1.2. The Concept of Identification by Using Self-Oscillations

If a process is closed in a loop with a nonlinear element as shown in Fig. 1, and given that the initial state of the process or the closed-loop input has enough energy, the system can enter a nonlinear behavior called self-oscillations, (Vukic *et al.* 2003.). The assumption is that the self-oscillations are monoharmonic (filter hypothesis is satisfied).

The idea of using self-oscillations for process identification resides on finding a connection between the self-oscillations' magnitudes and frequencies, and process parameters. This connection can be found by using the Goldfarb method, (Vukic *et al.* 2003), given with equation (1),

$$G_P(j\omega) = -\frac{1}{G_N(X_m)} = -\frac{1}{P_N(X_m) + jQ_N(X_m)} \qquad (1)$$

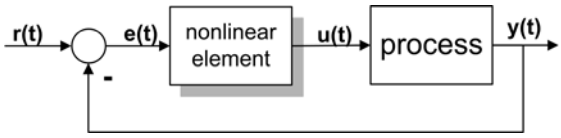

Fig. 1. Closed-loop scheme for inducing self-oscillations.

where $G_N(X_m)$ is the describing function , X_m is the magnitude of oscillations at the input of the nonlinear element and $G_P(j\omega)$ is the process frequency characteristic. Equation (1) can be graphically interpreted as finding intersection points between Nyquist frequency characteristic of the LTI process and an inverse negative describing function of the nonlinear element. Some prior work on using self-oscillations to determine system's parameters can be found in (Luyben, 1987), (Li *et al.*, 1991), (Chang and Shen, 1992), (Wang *et al.*, 1999) and references within. Usually, the nonlinear element that is used is a relay with hysteresis because it can induce self-oscillations for any process whose Nyquist curve passes through the third quadrant. The describing function of the relay with hysteresis is given with (2) where x_a is half the width of the hysteresis, and C is the relay output.

$$\begin{aligned} P(X_m) &= \frac{4C}{\pi X_m}\sqrt{1-\left(\frac{x_a}{X_m}\right)^2} \\ Q(X_m) &= -\frac{4C}{\pi X_m^2}x_a \end{aligned} \qquad (2)$$

Once the self-oscillations are established in a closed loop system, we can use the magnitude and frequency of the obtained self-oscillations at the input of the nonlinear element and determine one point in the Nyquist plane which is also one point on the Nyquist curve of the process. Depending on the number of the unknown process parameters, more different self-oscillations may be obtained. For more details, the reader is referred to (Miskovic *et al.*, 2007).

2. ALGORITHM DESCRIPTION

The algorithm will be derived for the case of a constant and linear drag model given with equations (3) and (4).

$$I_{\dot{r}}\dot{r} + k_r r = \tau \qquad (3)$$

$$I_{\dot{r}}\dot{r} + k_{r|r|} r|r| = \tau \qquad (4)$$

In the first case, differential equation describing the motion is linear, while in the second it is nonlinear.

1.1. Linear case

A general LTI system can be written by the following form:

$$G_P(s) = \frac{\sum_{i=0}^{m} b_i s^i}{\sum_{i=1}^{n} a_i s^i + 1}. \tag{5}$$

A general identification algorithm by use of self-oscillations appropriate for system (5) can be found in (Miskovic et al. 2007b). The short version is described here. The linear system parameters an be found using equation $\underbrace{\left[\boldsymbol{\Omega}_a \,|\, \boldsymbol{\Omega}_b\right]}_{\boldsymbol{\Omega}} \boldsymbol{\Theta} = \underbrace{\begin{bmatrix} -\underline{\mathrm{I}} \\ \underline{0} \end{bmatrix}}_{\mathbf{Y}}$ where $\boldsymbol{\omega} = \left[\omega_1 \cdots \omega_\varepsilon\right]^T$; $\mathbf{P} = \left[P_1 \cdots P_\varepsilon\right]^T$ and $\mathbf{Q} = \left[Q_1 \cdots Q_\varepsilon\right]^T$ are measurement vectors with elements P_i and Q_i being functions of the experimentally obtained magnitude of self-oscillations and nonlinear elements parameters, and ω_i frequency of the self-oscillations obtained in the ith experiment, vector of unknown parameters is $\boldsymbol{\Theta} = \left[\boldsymbol{\Theta}_a \; \boldsymbol{\Theta}_b\right]^T = \left[a_1 \cdots a_n \,|\, b_0 \cdots b_m\right]^T$.

$$\boldsymbol{\Omega}_a = \begin{bmatrix} \mathbf{0}_\varepsilon & -\mathbf{I}_\varepsilon & \mathbf{0}_\varepsilon & \mathbf{I}_\varepsilon \\ \mathbf{I}_\varepsilon & \mathbf{0}_\varepsilon & -\mathbf{I}_\varepsilon & \mathbf{0}_\varepsilon \end{bmatrix} \begin{bmatrix} \boldsymbol{\omega}.^1 & \underline{0} & \underline{0} & \underline{0} & \cdots & \neg(n-1)\%4 \cdot \boldsymbol{\omega}.^n \\ \underline{0} & \boldsymbol{\omega}.^2 & \underline{0} & \underline{0} & \cdots & \neg(n-2)\%4 \cdot \boldsymbol{\omega}.^n \\ \underline{0} & \underline{0} & \boldsymbol{\omega}.^3 & \underline{0} & \cdots & \neg(n-3)\%4 \cdot \boldsymbol{\omega}.^n \\ \underline{0} & \underline{0} & 0 & \boldsymbol{\omega}.^4 & \cdots & \neg(n-4)\%4 \cdot \boldsymbol{\omega}.^n \end{bmatrix}$$

$$\boldsymbol{\Omega}_b = \begin{bmatrix} \mathbf{P}^T & \mathbf{Q}^T \\ \mathbf{Q}^T & -\mathbf{P}^T \end{bmatrix} \begin{bmatrix} \mathbf{I}_\varepsilon & \mathbf{0}_\varepsilon & -\mathbf{I}_\varepsilon & \mathbf{0}_\varepsilon \\ \mathbf{0}_\varepsilon & -\mathbf{I}_\varepsilon & \mathbf{0}_\varepsilon & \mathbf{I}_\varepsilon \end{bmatrix} \begin{bmatrix} \boldsymbol{\omega}.^0 & \underline{0} & \underline{0} & \underline{0} & \cdots & \neg m\%4 \cdot \boldsymbol{\omega}.^m \\ \underline{0} & \boldsymbol{\omega}.^1 & \underline{0} & \underline{0} & \cdots & \neg(m-1)\%4 \cdot \boldsymbol{\omega}.^m \\ \underline{0} & \underline{0} & \boldsymbol{\omega}.^2 & \underline{0} & \cdots & \neg(m-2)\%4 \cdot \boldsymbol{\omega}.^m \\ \underline{0} & \underline{0} & \underline{0} & \boldsymbol{\omega}.^3 & \cdots & \neg(m-3)\%4 \cdot \boldsymbol{\omega}.^m \end{bmatrix}$$

and $\mathbf{I}_\varepsilon = \mathbf{I}_{\varepsilon\times\varepsilon}$, $\mathbf{0}_\varepsilon = \mathbf{0}_{\varepsilon\times\varepsilon}$, $\underline{0} = \mathbf{0}_{\varepsilon\times 1}$, $\underline{\mathrm{I}} = \mathbf{I}_{\varepsilon\times 1}$. The dot symbol ($.^k$) denotes the element-wise exponent, % is the modulus operation and $\neg$ is the logical negation symbol. The parameter vector $\boldsymbol{\theta}$ can be found by using the formula $\boldsymbol{\Theta} = \boldsymbol{\Omega}^{-1}\mathbf{Y}$ only if there is an even number of unknown parameters. If there is an odd number of parameters, matrix $\boldsymbol{\Omega}$ will have one row more than there are parameters. In this case, the last row can simply be omitted, or the pseudo-inversion can be used.

For the case of an ROV with the assumption of the linear model in the form of $I_r\ddot{\psi} + k_r\dot{\psi} = \tau$, the following transfer function can be written

$$\frac{\psi(s)}{\tau_N(s)} = \frac{\frac{1}{k_r}}{s\left(\frac{I_r}{k_r}s + 1\right)} = \frac{b_0}{s\left(a_1 s + 1\right)} \tag{6}$$

Using the proposed identification algorithm for linear systems we get

$$\boldsymbol{\Omega}_a = \begin{bmatrix} 0 \\ \omega \end{bmatrix} \qquad \boldsymbol{\Omega}_b = \begin{bmatrix} P \\ Q \end{bmatrix}.$$

Since the system has one integrator, the following modification has to be made upon the describing function vector, (Miskovic *et al.*, 2007b)

$$\begin{bmatrix} P^* \\ Q^* \end{bmatrix} = \begin{bmatrix} 0 & \omega^{-1} \\ -\omega^{-1} & 0 \end{bmatrix} \begin{bmatrix} P \\ Q \end{bmatrix} = \begin{bmatrix} Q/\omega \\ -P/\omega \end{bmatrix}$$

giving matrix equation

$$\begin{bmatrix} 0 & Q/\omega \\ \omega & -P/\omega \end{bmatrix} \begin{bmatrix} a_1 \\ b_0 \end{bmatrix} = \begin{bmatrix} -1 \\ 0 \end{bmatrix}$$

which yields the following linear equation parameters:

$$k_r = -\frac{Q}{\omega}, \qquad I_r = \frac{P}{\omega^2}.$$

1.2. Nonlinear case

In the case where the yaw model of an underwater vehicle can be described by using nonlinear dynamics given with (4), then the parameters can be determined using the following procedure.

If the system is in oscillatory regime, then the following equations can be written, under the assumption that the oscillations are symmetric:

$$\begin{aligned} \psi &= X_m \sin(\omega t) \\ \dot{\psi} &= X_m \omega \cos(\omega t) = jX_m \omega \sin(\omega t) \\ \ddot{\psi} &= -X_m \omega^2 \sin(\omega t) \end{aligned} \tag{7}$$

Combining (4) and (7) yields the following equation:

$$\begin{aligned} & I_r\left[-X_m\omega^2 \sin(\omega t)\right] + k_{r|r|}\left[X_m^2\omega^2 \cos(\omega t)\left|\cos(\omega t)\right|\right] \\ & = G_N\left[X_m \sin(\omega t)\right] \end{aligned}$$

$$\cos(\omega t)\left|\cos(\omega t)\right| \approx \frac{8}{3\pi}\cos(\omega t) = j\frac{8}{3\pi}\sin(\omega t)$$

The multiplication of the two cosine terms can be developed into a Fourier series (in the same manner as the describing function is derived, see (Vukic *et al.* 2003.)), which gives equation (8).

$$-I_r X_m \omega^2 + k_{r|r|} X_m^2 \omega^2 j\frac{8}{3\pi} = -G_N X_m \tag{8}$$

From equation (8), drag coefficient and moment of inertia can be determined using (9) and (10).

$$I_r = \frac{P_N}{\omega^2} \tag{9}$$

$$k_{r|r|} = -\frac{Q_N}{X_m\omega^2}\frac{3\pi}{8} \tag{10}$$

From this it is obvious that the term for the moment of inertia in the linear and nonlinear case are the same, while the expressions for the drag coefficient differ. This calculus shows that by using a simple identification procedure by use of self-oscillations can yield an UUV model that can be used for autopilot design.

1.3. Proof of Self-Oscillations Symmetry

One of the assumptions that are made while performing proposed identification experiments is that the self-oscillations of the system are symmetric. In (Miskovic *et al.*, 2006) a proof is given that a constantly excited system composed of a symmetric nonlinear element and a Type 1 (or higher) process, produces symmetric oscillations at the input of a nonlinear element. Here we give proof of self oscillation symmetry for a wider class of processes, including processes with nonlinear damping.

Theorem:
A constantly excited system composed of a symmetric nonlinear element, a Type 1 (or higher) process and a symmetric damping, produces symmetric oscillations at the input of a nonlinear element.

Proof:
A general system described above can be written in the following form

$$a\ddot{x} + F(\dot{x}) = \tau \tag{11}$$

where x is the process' output, $F(\dot{x})$ is the process' damping and τ is the process' input. Fourier series development of static nonlinearity $F(\dot{x})$ gives

$$\begin{aligned} F(\dot{x}) &= a_0 + \sum_{n=1}^{\infty} a_n \sin(nt) + \sum_{n=1}^{\infty} b_n \cos(nt) = \\ &\approx a_0 + a_1 \sin(t) + b_1 \cos(t) = \\ &= a_0 + (a_1 + jb_1)\sin(t) \end{aligned} \quad . \tag{12}$$

If damping is symmetric, Fourier series (12) do not have a constant term, i.e. $a_0 = 0$. Let's make an assumption that the induced oscillations are asymmetric, i.e.

$$\begin{aligned} x(t) &= x_0 + X_m \sin(\omega t) \\ \dot{x}(t) &= X_m \omega \cos(\omega t) \\ \ddot{x}(t) &= -X_m \omega^2 \sin(\omega t) \end{aligned} \quad . \tag{13}$$

From this, system (11) in self-oscillations regime can be described with the following equation.

$$\begin{aligned} -aX_m\omega^2 \sin(\omega t) + (a_1 + jb_1)\sin(\omega t) \\ = G_N\left[x_0 + X_m \sin(\omega t)\right] \end{aligned} \tag{14}$$

This equation has a solution if and only if $x_0 = 0$. QED

2. ERROR ANALYSIS

The initial assumption made on self-oscillations method is that they are monoharmonic. This is not true in real systems – nonlinear systems produce higher harmonics. This assumption can be true if the magnitude of higher harmonics is substantially smaller than the magnitude of smaller harmonics. One approach would be filtering the obtained self-oscillations. This, however, can require larger datasets or more demanding calculus, i.e. computational power. This is why we present an a priori error analysis for linear and nonlinear UUV models.

The error in determining drag coefficient, ε_{k_r} and $\varepsilon_{k_{r|r|}}$, and moment of inertia, $\varepsilon_{I_{\dot{r}}}$, versus $\frac{X_m}{x_a}$ ratio for linear and nonlinear model are shown in Fig. 2. in red crosses and blue circles, respectively. The error is obviously smaller in the linear case, since the only element whose approximation causes the error is the nonlinear element. In the nonlinear case, the process itself is approximated by using Fourier series, hence the error is larger. An important thing that should be stressed out is that the curves in Fig. 1 do not depend on the process parameters. The importance of this is that the given error functions are valid for any system that can be described using equations (3) and (4) (does not depend on system's parameters).

Using the results in Fig. 2, we can conclude that the error in determining moment of inertia is quite small in all cases. However, the error in determining drag coefficient can be significant. These simulation results show that if the experimentally obtained magnitude of oscillations is around 1.5 times the width of the hysteresis, the error will be small.

As it was mentioned earlier, the error occurs due to different values of calculated magnitude ($\bar{X}_m$) and frequency ($\bar{\omega}$) of self-oscillations, and the obtained ones, (X_m and ω). The errors ε_{k_r}, $\varepsilon_{k_{r|r|}}$ and $\varepsilon_{I_{\dot{r}}}$ can be written as functions of ratios of real and obtained magnitudes, γ_x, and frequencies γ_ω (see equations (15), (16) and (17)). The mentioned ratios are shown in Fig 3. and are also the same for any system that can be described with equations (3) and (4).

$$\varepsilon_{I_r} = \left|\frac{I_r}{\bar{I}_r} - 1\right| = \left|\gamma_\omega^2 \gamma_x \sqrt{\frac{\left(\frac{X_m}{x_a}\right)^2 - 1}{\left(\frac{X_m}{x_a}\right)^2 - \frac{1}{\gamma_x^2}}} - 1\right| \quad (15)$$

$$\varepsilon_{k_{rr}} = \left|\frac{k_{rr}}{\bar{k}_{rr}} - 1\right| = \left|\gamma_x^3 \gamma_\omega^2 - 1\right| \quad (16)$$

$$\varepsilon_{k_r} = \left|\frac{k_r}{\bar{k}_r} - 1\right| = \left|\gamma_x^2 \gamma_\omega - 1\right| \quad (17)$$

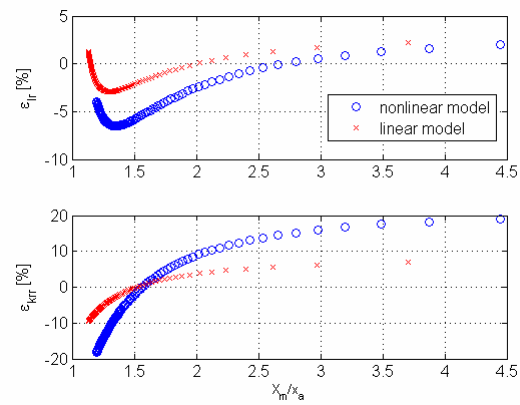

Fig. 2. Errors in determining drag coefficient and moment of inertia.

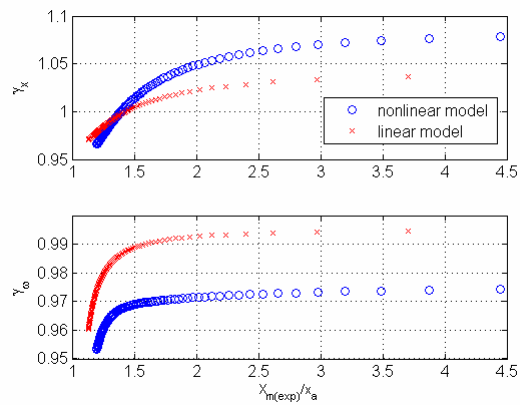

Fig. 3. Ratios between the obtained and real self-oscillation magnitudes and frequencies.

3. EXPERIMENTAL RESULTS

The proposed algorithm for linear and nonlinear identification has been performed on an AUV built

Table 1 Yaw models' parameters identified using open-loop procedures

Model	*linear*	*nonlinear*
$k_{r\|r\|}$	-	1.257
k_r	0.9961	-
$I_{\dot{r}}$	0.7058	1.018

Table 2 Experimentally obtained data

C	x_a [°]	x_a^* [°]	X_{max} [°]	X_{min} [°]	T_H [s]	T_L [s]
1	20	23.8	38	-38.4	2.54	2.34

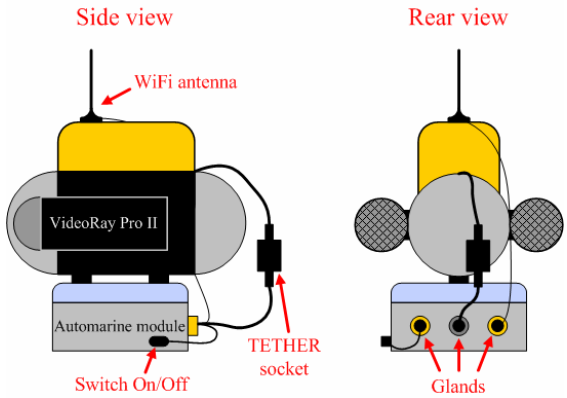

Fig. 4. The *Automarine Module* installation.

Table 3 Yaw models' parameters identified using the proposed procedure

Model	*linear*	*nonlinear*
$k_{r\|r\|}$	-	1.2661
k_r	0.9233	-
$I_{\dot{r}}$	0.8995	0.8995

from a VideoRay Pro II ROV and *Automarine* module (see Fig. 4.). For details on the construction of this system, the reader is referred to (Stipanov *et al.*, 2007).

This systems yaw model parameters have been identified using open-loop procedures, and the results are given in table 1. The validation of these parameters is also given in (Stipanov *et al.*, 2007). We have shown that the nonlinear model describes the system better. For the sake of algorithm testing, we will also provide the results of the identification of the linear model of the system.

Table 2 gives parameters of the relay that was used in the experiment of obtaining self-oscillations, together with the results. Parameter C is the applied normalized torque, x_a is the set hysteresis width, x_a^* is modified hysteresis width (Miskovic *et al.* 2007b), X_{max} and X_{min} are the maximum and minimum of the obtained self-oscillations respectively, and T_H and T_L are the durations of the hysteresis high and low state respectively. Finally, table 3 gives the identified parameters, using the proposed method based on self-oscillations.

The results show that this method gives accurate results. The main advantage of this method is that it is not time consuming. While for performing open loop

experiments a great number of data has to be obtained, in this method only a couple of similar oscillations must be recorded in order to determine the model's parameters. In this particular case, oscillation period is about 5s, and 5 periods were taken into account – the identification procedure took less than 30[s]! Another advantage is that, since the procedure is performed in closed-loop, the disturbance influence is much smaller than in the case of system identification in open-loop. It should be mentioned that this method can be applied to other degrees of freedom of an underwater vehicle, which can be described using similar models.

4. CONCLUSION

In this paper we presented a method for determining linear and nonlinear yaw model parameters by using self-oscillations. The novel approach is in use of the general matrix formed algorithm presented in (Miskovic et al., 2007b) and the use of the procedure for nonlinear systems. We also gave error analysis with recommendations on when the error will be the smallest. The experiments were performed on an AUV which consists of a VideoRay Pro II ROV and an *Automarine* module. Comparison of the obtained results with the results from an open-loop identification procedure, prove the applicability and accuracy of the proposed method. The main advantage of this method is that it is not time consuming, and that due to the closed-loop procedure, the disturbance influence is minimized.

Future work will include determining analytical expressions for describing the ratio between the obtained magnitudes and frequencies of self-oscillations, and analytically derived values. Further on, we will give simulation and experimental identification results when the disturbance is present, proving the robustness of the system to external disturbances.

ACKNOWLEDGMENT

The work was carried out in the framework of the research project "*RoboMarSec* – Underwater robotics in sub-sea protection and maritime security" supported by the Ministry of Science, Education and Sport of the Republic of Croatia (Project No.036-0362975-2999).

REFERENCES

Caccia, M., Casalino, G., Cristi, R. and Veruggio, G. (1998). Acoustic motion estimation and control for an unmanned underwater vehicle in a structured environment, *Control Engineering Practice* **6**, 661-670.

Caccia, M., Indiveri, G. and Veruggio, G. (2000). Modelling and identification of open-frame variable configuration underwater vehicles, *IEEE Journal of Ocean Engineering* **25**(2), 227-240.

Carreras, M., Ridao, P., Garcia R. and Nicosevici, T. (2003). Vision-based localization of an underwater robot in a structured environment, *IEEE International conference on robotics and automation, ICRA'03*, Taipei, Taiwan

Chang, R. S. and Shen, C. Y. (1992). Derivation of transfer function from relay feedback systems, *Ind. Eng. Chem. Res.*, **31**, 855.

Fossen, T.I. (1994). *Guidance and Control of Ocean Vehicles*.

Li, W., Eskinat, E. and Luyben, W. L. (1991). An improved autotune identification method, *Ind. Eng. Chem. Res.*, **30**, 1530.

Ljung, L. (1999). *System Identification – Theory for the user*, 2nd ed., Prentice Hall.

Luyben, W. L. (1987). Derivation of transfer functions for highly nonlinear distillation columns, *Ind. Eng. Chem. Res.*, **26**, 2490.

Miskovic, N., Vukic, Z., Barisic, M. and Tovornik, B. (2006). Autotuning autopilots for micro-ROVs, *Proceedings of the 14th Mediterranean Conference on Control and Applications*, Ancona, Italy.

Miskovic, N., Vukic, Z. and Barisic, M. (2007a). Identification of coupled mathematical models for underwater vehicles, *Proceedings of the OCEANS'07 Conference*, Aberdeen, Scotland.

Miskovic, N., Vukic, Z. and Barisic, M. (2007b). Transfer function identification by using self-oscillations, *Proceedings of the 15th Mediterranean Conference on Control and Applications*, Athens, Greece.

Ridao, P., Tiano, A., El-Fakdi, A., Carreras, M., and Zirilli, A. (2004). On the identification of non-linear models of unmanned underwater vehicles, *Control Engineering Practice* **12**, 1483-1499.

Stipanov, M. (2007). *Autonomization of the VideoRay Pro II remotely operated submersible*, master thesis, University of Zagreb, Faculty of Electrical Engineering and Computing, (in Croatian).

Stipanov M., Miskovic, N., Vukic, Z. and Barisic, M. (2007). ROV autonomization – yaw identification and Automarine module architecture, *Proceedings of the CAMS'07 Conference*, Bol, Croatia.

Vukic, Z., Kuljaca, Lj., Donlagic, D. and Tesnjak, S. (2003). *Nonlinear control systems*. Marcel Dekker. New York.

Vukic, Z. and Kuljaca, Lj. (2005). *Automatic control – analysis of linear systems*. Kigen. Zagreb (in Croatian)

Wang, L., Desarmo, M. L. and Cluett, W.R. (1999). Real-time estimation of process frequency response and step response from relay feedback experiments, *Automatica*, **35**, 1427.